Membrane-Type 4 Matrix Metalloproteinase promotes breast cancer growth and metastases

Vincent Chabottaux,[1] Nor Eddine Sounni,[1] Caroline J. Pennington,[2] William R. English,[3] Frédéric van den Brûle,[1, 4] Silvia Blacher,[1] Christine Gilles,[1] Carine Munaut,[1] Erik Maquoi,[1] Carlos Lopez-Otin,[5] Gillian Murphy,[3] Dylan R. Edwards,[2] Jean-Michel Foidart,[1, 4] and Agnès Noël[1]

[1]Laboratory of Tumor and Development Biology, University of Liège, Sart Tilman B23, Centre de Recherche en Cancérologie Expérimentale (CRCE), Center for Biomedical Integrative Genoproteomics (CBIG), B-4000 Liège, Belgium; [2]School of Biological Sciences, University of East Anglia, Norwich, NR4 7TJ, Norfolk, United Kingdom; [3]Department of Oncology, Cambridge Institute for Medical Research, Cambridge University, Cambridge CB2 2XY, United Kingdom; [4]Department of Gynecology, CHU, B-4000 Liège; [5]Departamento de Bioquímica y Biología Molecular, Facultad de Medicina, Instituto Universitario de Oncología, Universidad de Oviedo, 33006-Oviedo, Spain.

Running Title: MT4-MMP promotes tumor growth and metastases

Key Words: MMP, angiogenesis, breast cancer, metastases, degradome

Corresponding author:

A NOEL

Laboratory of Tumor and Development Biology

University of Liège, Tour de Pathologie (B23), Sart-Tilman, B-4000 Liège

Tel : +32-4-366.24.53.

Fax: +32-4-366.29.36.

E-mail: agnes.noel@ulg.ac.be

ABSTRACT

Membrane-type matrix metalloproteinases (MT-MMPs) constitute a subfamily of 6 distinct membrane-associated MMPs. Although the contribution of MT1-MMP during different steps of cancer progression has been well documented, the significance of other MT-MMPs is rather unknown. We have investigated the involvement of MT4-MMP, a glycosylphosphatidyl-inositol (GPI) anchored protease in breast cancer progression. Interestingly, immunohistochemical analysis demonstrates that MT4-MMP production at protein level is strongly increased in epithelial cancer cells of human breast carcinomas as compared to normal epithelial cells. Positive staining for MT4-MMP is also detected in lymph node metastases. In contrast, quantitative RT-PCR analysis reveals similar MT4-MMP mRNA levels in human breast adenocarcinomas and normal breast tissues. Stable transfection of MT4-MMP cDNA in human breast adenocarcinoma MDA-MB-231 cells does not affect *in vitro* cell proliferation or invasion, but strongly promotes primary tumor growth and associated metastases in RAG-1 immunodeficient mice. We provide for the first time evidence that MT4-MMP over-production accelerates *in vivo* tumor growth, induces enlargement of intratumoral blood vessels and is associated with increased lung metastases. These results identify MT4-MMP as a new putative target to design anti-cancer strategies.

INTRODUCTION

Matrix Metalloproteinases (MMPs) are a family of zinc-binding endopeptidases that can degrade virtually all extracellular matrix components as well as a growing number of other modulators of cell functions (1-4). Although most MMPs are secreted as soluble enzymes, 6 of them are membrane-type MMPs (MT-MMPs) which are associated with the cell membrane by either a transmembrane domain (MT1-, MT2-, MT3-, MT5-MMPs) or a glycosylphosphatidyl-inositol (GPI) anchor (MT4-, MT6-MMPs) (5).

MT1-MMP, the first discovered member of this subfamily, was initially described as an activator of pro-MMP2 (6). MT1-MMP plays critical roles in cell migration, cell invasion, physiological and pathological remodeling of ECM (5, 7). It is a multifunctional protease for which an increasing number of substrates have been identified, including pro-MMP2, pro-MMP13, extracellular matrix components, cell surface receptors, growth factors, chemokines, adhesion and signaling molecules (2, 5). Its implication in tumor growth, invasion and angiogenesis is now well documented (5, 8-11). A pro-angiogenic effect of MT1-MMP has been linked, at least in part, to an up-regulation of vascular endothelial growth factor (VEGF) (12, 13).

Although much emphasis has been placed on understanding the biochemical features and functions of MT1-MMP (5), little attention has been given to the implication of other MT-MMPs in cancer progression and angiogenesis. Different MT-MMPs (MT2-, MT3-, MT5-MMPs) can activate pro-MMP2 but less efficiently than MT1-MMP (5, 14, 15). Despite being able to bind TIMP-2 (tissue inhibitor of metalloproteinase-2), MT4- and MT6-MMPs are rather inefficient at activating pro-MMP2 (16-18). Since its original isolation from human breast carcinoma (19), MT4-MMP has been detected in several human cancers, including gliomas (20), prostate (21) and breast carcinomas (19). However, its localization and implication during human breast cancer progression is currently unknown. The inability of MT4-MMP to activate

pro-MMP2 and the lack of a cytoplasmic tail in this cell surface GPI-anchored protease suggests that MT4-MMP displays different functions than MT1-MMP. Its few known substrates are fibrinogen, fibrin and proTNF-α and ADAMTS-4 (a disintegrin and metalloproteinase with thrombospondin-like motif-4) (16, 22, 23).

The aim of this study was to explore the expression of MT4-MMP in human breast carcinomas by RT-PCR and immunohistochemical analyses and to investigate its putative role in cancer progression through its over-expression in human breast adenocarcinomas cells. We provide evidence that MT4-MMP is produced at higher levels by human mammary carcinoma cells than by normal epithelial cells. We demonstrate for the first time that its over-expression in human breast cancer cells promotes primary tumor growth leading to increased lung metastases. A link between MT4-MMP and metastatic dissemination of human breast cancers is further supported by its strong expression in human lymph node metastases.

MATERIAL AND METHODS

Human tissue samples

Human breast samples were obtained from tumor banks of Center for Experimental Cancer Research (University of Liège) and of School of Biological Sciences, University of East Anglia (United Kingdom). Breast tumor samples were obtained from 63 patients with invasive breast ductal carcinomas who underwent surgery. Normal breast tissues were obtained from 21 patients who underwent reduction mammoplasty. Twelve metastatic and 6 normal lymph nodes from 4 patients were also collected. Breast tumors were reviewed regarding histopathologic type based on the World Health Organization (WHO) classification. All cancer samples were characterized by more than 70 % cancer cell composition. Total RNA was extracted from frozen samples with RNeasy Mini Kit (QIAGEN GmbH, Hilden, Germany) according to manufacturer's instructions.

Cell culture

Human breast cancer MDA-MB-231 cells obtained from American Type Culture Collection (Manassas, VA) were grown to 80% confluence in Dulbecco's Modifed Eagle's Medium (DMEM) supplemented with 10% fetal calf serum (FCS), 2 mM L-glutamine, 100 U/ml of penicillin and 100 µg/ml of streptomycin at 37°C in a 5% CO2 humid atmosphere. All culture reagents were purchased from Gibco-Life Technologies (Invitrogen Corporation, Paisley, Scotland).

Stable transfection of MDA-MB-231 cells with human MT4-MMP cDNA

Parental MDA-MB-231 cells were stably transfected by electroporation (250 V, 960 µF) with pcDNA3-*neo* vector containing only the neomycin resistance gene (control plasmid) or with the same plasmid carrying the full-length human MT4-MMP cDNA (pcDNA3-MT4) (19, 24). Selection was performed under G418 pressure (1.5 mg/ml) (Life Technologies) and

screening of clones was based on RT-PCR analysis to determine MT4-MMP expression. Stable transfectants were maintained in medium containing G418 (500 µg/ml).

Preparation of proteins cell extracts, conditioned media and total RNAs

Conditioned media of cells for ELISA were prepared by seeding cells (2.5×10^5) onto 6 well-plates for 24 h in 3 ml of DMEM with serum, followed by incubating cells for 48 h in 1.5 ml of serum-free DMEM. Similarly, conditioned media for rat aortic rings assay were prepared by culturing 10^6 cells in 100 mm diameter Petri dishes (Falcon, Beckton Dickinson, Lincoln Park, New Jersey). Cells were grown in 8 ml of DMEM with serum for 24 h and then, in 6 ml of serum-free DMEM for 48 h. Conditioned media were harvested, clarified by centrifugation and stored frozen at -20°C. Total protein cell extracts were prepared from cell monolayers incubated in RIPA buffer (25). Protein concentration was determined by using the DC protein Assay Kit (Bio-rad Laboratories, Hercules, CA). Total RNAs were extracted from cell monolayer using High Pure RNA isolation kit (Roche Diagnostic Applied Science, Mannheim, Germany).

Semi-quantitative Reverse Transcriptase-PCR analysis

RT-PCR was performed on 10 ng of total RNA extracted from cells using a GeneAmp Thermostable r*Tth* Reverse Transcriptase RNA PCR kit (Applied Biosystems, Foster City, CA) following manufacturer's instructions. Specific pairs of primers (Eurogentec, Seraing, Belgium) for human MT4-MMP were designed as follows: forward 5'-AAGGAGACAGGTACTGGGTGTTC-3'; reverse 5'-TCGCCATCCAGCACTTTCCAGTA-3'. Cycles (36) of amplification were run for 15 s at 94 °C, 20 s at 68 °C and 30 s at 72 °C.

Quantitative Reverse Transcriptase-PCR analysis

Reverse Transcription and Quantitiative RealTime PCR were conducted as described in Nuttall *et al*. (20). Sequences for the primers and the probe specific to MT4-MMP were designed as follows: forward 5'-GCGGGTATCCTTCCTCTACGT-3'; reverse 5'-

CAGCGACCACAAGATCGTCTT-3'; probe 5'-FAM-ATTGTCCTTGAACACCCAGTAC CTGTCTCCTTTAA-TAMRA-3'.

Western blotting analysis

Samples (20 µg of total cell protein extracts) were separated under reducing conditions on 10 % polyacryamide gels and transferred onto PVDF membranes (NEN, Boston, MA). Membranes were blocked overnight at 4 °C with Gloria milk powder (5 %, w/v), Tween 20 (0.05 %, v/v) in phosphate buffered saline (PBS). Antigenic bands were detected by exposing the membranes to primary antibody [anti-human MT4-MMP sheep polyclonal antibody (16) or anti-MT1-MMP mouse monoclonal antibody (12)], followed by incubation with a secondary horseradish peroxidase (HRP)-conjugated rabbit anti-sheep antibody or goat anti-mouse antibody (1:1,000, DakoCytomation, Glostrup, Denmark). Signals were detected using an enhanced chemiluminescence (ECL) kit (PerkinElmer Life Sciences, Boston, MA), according to manufacturer's instructions and actin production level was determined as loading control.

***In vitro* growth rate**

MDA-MB-231 cells (10^4) were seeded in triplicate in 24-well plates and maintained in standard culture conditions. Fluorimetric DNA titration was performed on samples harvested every day and used as an indicator of cell density (26). The average cell density from triplicate experiments was determined as a function of time.

In vitro invasion assay: Boyden chamberCell invasion was assayed using a Transwell cell culture chamber inserts system (Costar, NY) with 6.5-mm polycarbonate filters (8 µm pore size) as previously described (25). Briefly, 6×10^4 cells were allowed to migrate through inserts, pre-coated with 25 µg of matrigel, for 20h. Cells having reached the lower surface of the filters were stained with Giemsa and counted in 30 random fields per insert (400-fold magnification). Each clone was tested three times in triplicate.

Enzyme-linked immunosorbent assay for quantitative determination of VEGF

VEGF ($VEGF_{165}$ and $VEGF_{121}$ isoforms) levels were determined in 100 µl of conditioned media (dilution 1:4) in triplicate using a human VEGF DuoSet ELISA development kit (R&D Systems, Minneapolis, MN) following manufacturer's instructions. VEGF amounts were normalized to total protein concentration of conditioned media.

***In vitro* angiogenesis: mouse aortic rings assay with conditioned media**

In vitro angiogenesis was studied by culturing rings of rat aorta in three-dimensional collagen gels as previously described (25). Images were captured on a Zeiss microscope at day 6 and morphometric analysis was performed on a "Sun SPARC30" workstation with the software "Visilog 5.0" from Noesis. After generating binary images, the number and the maximal length of the outgrown microvessels were automatically performed (27).

***In vivo* tumorigenicity**

Subconfluent MDA-MB-231 cells were trypsinized, resuspended in serum-free medium (5×10^6 cells/ml) and mixed with an equal volume of cold Matrigel according to Noël *et al.* (28). Cell suspension (10^6 cells in 400 µl) was injected subcutaneously into RAG-1 immunodeficient mice (29) at both flanks (5 or 6 mice/clone in each assay). Tumor growth was assessed by measuring the length and width of tumors every 3-4 days. Tumor volumes were estimated using the formula (length) X $(\text{width})^2$ X 0.4 (28). Results are expressed as the mean of tumor volumes for each experimental group. Tumor incidence represents the percentage of mice bearing tumor larger than 200 mm^3 at day 45.

Immunohistochemistry

To unmask antigens on paraffin sections (5-µm thick), slides were incubated for 1 hr at 80 °C in citrate buffer pH6 (Dako, Glostrup, Denmark, S2031), autoclaved for 11 min at 126 °C in Target Retrieval Solution (Dako, S1699) or in citrate buffer (pH6), micro-waved for 4 x 5 min at 350 W in Target Retrieval Solution for MT4-MMP, Ki-67, α-smooth muscle actin (SMA), von Willebrand factor (vWF) stainings, respectively. Endogenous peroxydase was

subsequently blocked by 3 % H_2O_2/ H_2O for 20 min and non-specific binding was prevented by incubation in PBS/BSA 10 % (Fraction V, Acros Organics, NJ) for 1 h (for MT4-MMP and Ki-67) or in normal goat serum for 30 min (for SMA and vWF). Sections were then incubated with a rabbit polyclonal anti-MT4-MMP (Sigma, M3684, 1:300) overnight at 4 °C, a mouse monoclonal anti-Ki-67 (Dako, clone MIB-1, M7240, 1:100), a mouse monoclonal anti-SMA (Dako, M0801, 1:100) or a rabbit polyclonal anti-vWF (Dako, A00602, 1:200) for 1 hr at room temperature (RT). Slides were then incubated with a HRP-conjugated second antibody (Envision System Labeled Polymer-HRP, Dako, K4001, ready to use) (for Ki-67) or with a biotinylated second antibody (Dako, E0433, 1:400) at room temperature for 30 min, followed by incubation with a Strepatavidin/HRP complex (Dako, P0397, 1:500) at RT for 30 min (for MT4-MMP, SMA and vWF). Coloring was performed with 3-3'diaminobenzidine hydrochloride (DAB, Dako, K3468) for 3 min. Slides were finally counter-stained with hematoxylin and mounted with Eukitt medium for microscope observation. Omission of the first antibody served as negative control.

Quantification of MT4-MMP production in human breast cancer

For quantitative measurement of MT4-MMP immunostaining, an original automatic computer-assisted image analysis was applied on 50 representative sections by using software "Aptelion 3-2" from Adsis. Staining density was determined by measuring the ratio between the surface of immunostaining and the surface of total mammary epithelium. The staining intensity (1/µm2) is defined as the sum of grey level intensities of each pixels characterizing stained region divided by surface of epithelium.

Lung metastasis assay from subcutaneous tumors

Paraffin sections of mice lung (5 mice/clones) were immuno-stained for human KI-67 protein (30). Metastatic foci were counted in 65 histological fields per section at 200-fold magnification. Incidence of metastasis is expressed as the percentage of mice with detectable

metastatic cells in the lungs. Severity of metastasis was scored as: minimal (score 1° = metastatic nodule involving less than 3 stained cells), medium (score 2° = metastatic nodule composed of 3 to 20 stained cells), or extensive involvement (score 3° = metastatic nodule including more than 20 stained cells).

Statistical analysis

We assessed statistical differences between both experimental groups using Mann-Whitney test. Fisher's exact test was used to compare metastasis incidences. In both tests, *P*-values < 0.05 (*) were considered as significant. Statistical analyses were carried out using the Prism 4.0 software (GraphPad, San Diego, CA).

RESULTS

MT4-MMP is produced by human breast epithelial cancer cells

MT4-MMP expression levels were first determined by real time qRT-PCR analysis in 63 breast adenocarcinomas and 21 normal breast tissue samples. MT4-MMP transcripts were expressed at similar levels in breast carcinomas and normal breast tissues (Fig. 1*A*). MT4-MMP production in human breast tissues was further investigated by immunohistochemistry revealing a strong homogenous staining of tumor cells in all breast tumor samples analyzed (n = 17) (Fig. 1*B*). Staining was detected in few interstitial cells presumably inflammatory cells (Fig. 1*B*). In normal breast tissues (n = 11), epithelial cells were stained at variable intensities ranging from a negative to a moderate positivity, myoepithelial cells being unreactive. Quantitative assessment of MT4-MMP staining was performed by computer-assisted image analysis. A strong enhancement of both density and intensity staining was observed in tumor samples (Fig. 1*C*).

Immunohistochemical analysis was also performed in normal and metastatic human breast cancer lymph nodes. Interestingly, in opposite to normal human breast lymph nodes, invading cancer cells as well as inflammatory cells of metastatic lymph nodes (11/12) were strongly immunostained for MT4-MMP (Fig. 1*B*).

The important MT4-MMP immunostaining of tumor epithelial cells in human cancer tissues prompted us to study the contribution of this membrane-associated enzyme in cancer progression and angiogenesis. Based on the mRNA expression profile of different human breast cancer cell lines (data not shown), MDA-MB-231 cells which expressed MT4-MMP at very low levels [in accordance with (19, 20, 31)] were selected for transfection with human MT4-MMP cDNA.

Generation of MDA-MB-231 cells stably expressing MT4-MMP

Parental MDA-MB-231 cells were stably transfected with control pcDNA3-*neo* vector (clones C) or with pcDNA3-*neo* containing human MT4-MMP cDNA (clones M). Four clones over-expressing MT4-MMP (M2, M3, M10, M14) and 4 control clones (C4, C12, C14, C15) were selected according to MT4-MMP expression at mRNA (Fig. 2*A*) and protein (Fig. 2*B*) levels. MT4-MMP over-expressing clones were found to stably express MT4-MMP. Western blot analysis revealed 2 bands at the expected molecular weight (~ 64 kDa), the upper one being the pro-form and the lower one being the active-form (16). Clone M2, which was characterized by the highest MT4-MMP production (Fig. 2) was confirmed to express both active- and pro-forms by loading a lower amount of protein in Western blot analysis. In all selected clones, MT1-MMP protein expression was not affected by transfection with MT4-MMP cDNA (data not shown).

MT4-MMP over-expression does not affect *in vitro* cell proliferation or invasion

Clones were then compared for their *in vitro* proliferation and invasive capacities through different matrices. MT4-MMP over-expression did not significantly affect *in vitro* growth rate as illustrated in Fig. 3*A* ($P > 0.05$). The *in vitro* invasion potential of all clones was then evaluated in Boyden chambers by using inserts coated with Matrigel. The numbers of invading cells was independent of MT4-MMP production ($P > 0.05$) (data not shown). Similarly, the capacity of MT4-MMP transfectants to migrate through gelatin-coated inserts or to invade type I collagen gel-coated inserts did not differ to that of control clones (data not shown).

Gelatin zymography (data not shown) revealed that MT4-MMP production by MDA-MB-231 clones, either treated or not with concanavalin-A, did not lead to a higher activation of exogenous pro-MMP2 [consistent with (16)].

MT4-MMP over-expression does not affect *in vitro* angiogenesis or VEGF expression

Since MT1-MMP has been demonstrated to affect *in vitro* and *in vivo* angiogenesis through a modulation of VEGF-A expression (12), we measured VEGF production of all clones by RT-PCR analysis and ELISA. VEGF mRNA levels in clones expressing MT4-MMP were undistinguishable from those of control clones (data not shown). Furthermore, similar amounts of proteins were detected by ELISA in medium conditioned by MT4-MMP over-expressing clones (1365 +/- 100 pg/ml) and control clones (1369 +/- 344 pg/ml). Similarly, RT-PCR analysis of other angiogenic molecules (VEGF-B, -C, -D and PlGF) did not reveal any difference between clones expressing or not MT4-MMP (data not shown).

In addition, we investigated the ability of selected clones to modulate *in vitro* angiogenesis in the rat aortic ring assay. Rat aortic rings were embedded in a collagen gel and maintained in MCDB supplemented with media conditioned by transfectants (1/6, v/v). After 6 days of incubation, computer-assisted image analysis was applied to determine geometrical and morphological parameters (number of vessels = Nv and maximal length of vessels = Lmax) (27). These parameters did not differ in aortic ring cultures supplemented with medium conditioned by cells expressing or not MT4-MMP (Nv = 26.5 +/- 5 for MT4-MMP clones *vs* 29 +/- 2 for control clones; Lmax = 614 µm +/- 46 for MT4 clones *vs* 543 µm +/- 40 for control clones).

MT4-MMP over-expression promotes *in vivo* primary tumor growth

RAG-1 immunodeficient mice were subcutaneously injected with the different MT4-MMP expressing or control clones in 3 separate sets of experiments. Tumor incidence and tumor growth were monitored from the third to the sixth week after injection. MT4-MMP over-expression resulted in increased tumor incidence and tumor growth (Fig. 3*B, C*). At day 45, tumor incidence was 96 % (46/48 tumors) in MT4-MMP expressing tumors and 50 % (19/38 tumors) in control tumors. Thirty-two days after cell injection, all tumors expressing MT4-MMP reached higher volumes as compared to control tumors ($P < 0.05$) (Fig. 3*B, C*). When

considering all independent experiments together, the mean tumor volumes reached at the end of the assays ranged from 639 to 1340 mm^3 for MT4-MMP-transfected cells, and from 54 to 486 mm^3 for control clones ($P < 0.05$).

Considering the previously described involvement of MT1-MMP in tumor angiogenesis (25), we further investigated whether MT4-MMP could affect tumor vascularization (Fig. 4*B*). No obvious difference in vessel density was detected between experimental groups. However, interestingly, MT4-MMP production affected vessel shape and size leading to an important enlargement of intratumoral blood vessels. Immunostaining for α-SMA revealed the presence of pericytes surrounding enlarged vessels of MT4-MMP expressing tumors, as well as collapsed and small vessels presenting a lumen in control tumors (Fig. 4*C*).

MT4-MMP over-expression is associated with an induction of lung metastases

Metastatic ability of all transfectants injected in RAG-1 -/- mice was assessed by histochemical and immunohistochemical analyses of lungs harvested 45 days after tumor cell inoculation. Numerous metastatic nodules were easily distinguishable in lungs of mice inoculated with MT4-MMP-expressing cells, but not in those of mice injected with control clones (Fig. 5*A*). In order to detect small metastatic foci, lung sections were immunostained with an antibody raised against human Ki-67 protein and detecting proliferative cancer cells (Fig. 5*A, B*). Incidence and severity of metastases were determined by considering the size of metastatic foci (number of cells/foci) (Table I). All clones over-expressing MT4-MMP induced lung metastasis in 100 % of injected animals. In sharp contrast, when considering control clones, metastasis incidence varied from 0 % to 100 % (Table I*A*). The severity of metastases was also strongly increased in mice injected with MT4-MMP expressing cells. Score 3° metastatic nodules (composed of more than 20 cells) were only detected after injection of MT4-MMP transfectants (Table I and Fig. 5*A*), while metastatic foci induced by inoculation of control clones were scored 1° (dispersed cells) or 2° (composed of less than 20 cells). In

addition, MT4-MMP transfectants showed a significant increase in the number of metastatic foci ($P < 0.05$) (Fig. 5*D*). When considering all clones together, it clearly appeared that both incidence and severity of metastasis were significantly higher in mice injected with MT4-MMP expressing clones as compared to control clones ($P < 0.001$). Immunohistochemistry further confirmed MT4-MMP expression in lung metastases produced by MT4-MMP transfected clones (Fig. 5*C)* as well as in the corresponding primary tumors (Fig. 4*A*).

DISCUSSION

We investigated the potential implication of the GPI-anchored MT4-MMP in breast cancer progression. This study provides the first direct evidence for a pivotal role of MT4-MMP in primary breast cancer growth leading to metastatic dissemination. Several lines of evidence support these conclusions. First, MT4-MMP is produced at higher levels in human breast cancer tissues than in normal breasts. Second, MT4-MMP over-expression in MDA-MB-231 cells resulted in an enhanced tumor incidence, in an acceleration of primary tumor growth with subsequent apparition of lung metastases and in an enlargement of intratumoral blood vessels. Third, the involvement of MT4-MMP in metastatic dissemination is suggested by its expression in human metastatic cells originating from human breast cancers.

Quantitative RT-PCR analyses were first performed on human normal breast and mammary adenocarcinoma samples. MT4-MMP mRNA was found expressed in all human breast adenocarcinoma samples, but at similar levels as in normal breast samples. However, interestingly, immunohistochemical analyses revealed a very high and homogenous production of MT4-MMP protein in human breast adenocarcinomas and metastatic lymph nodes, which is consistent with its original isolation from a human breast adenocarcinoma source (19). While MT1-MMP was described as a stromal MMP (32-34), MT4-MMP expression appears restricted to cancerous epithelial cells with some staining in inflammatory cells. Quantitative analysis revealed a 3 to 4 fold increase of MT4-MMP staining density and intensity in tumor samples as compared to normal breast tissues in which a faint and irregular immunostaining was observed. The absence of a correlation between MT4-MMP mRNA levels and tumor development might appear disappointing. However, this observation is consistent with previous studies performed on human prostate cancers (21) and mammary carcinomas of PyMT mice (transgenic for polyoma virus middle T antigen under the control of the MMTV promoter) (35). The discrepancy between RT-PCR and immunohistochemical results could be related to

mRNA heterogeneities of samples used for total RNA extractions, while tissue sections allow a better localization of the molecule of interest. In addition, MT4-MMP production could be controlled at post-transcriptional and/or post-translational levels. Increased production of MT4-MMP in tumors could be related to modification of mRNA translation rate or reduction of MT4-MMP degradation, cell surface shedding and/or internalization. Evidences exist indicating that members of MT-MMP subfamily can be internalized (36, 37) or shed from the cell membrane (5, 38). Dissection of molecular mechanisms leading to a regulation of MT4-MMP protein requires further investigations. Therefore the increased MT4-MMP protein production in human breast adenocarcinomas might suggest a specific function of MT4-MMP in human breast cancer progression and prompted us to evaluate the effect of MT4-MMP over-expression in human breast cancer cell lines.

We next transfected human breast cancer MDA-MB-231 cells with MT4-MMP cDNA. Four clones stably expressing this MT-MMP and four control clones were characterized *in vitro* and *in vivo*. Although MT4-MMP over-expression in MDA-MB-231 cells does not significantly affect their *in vitro* proliferation or *in vitro* invasiveness in the different matrices tested, it strongly increases their *in vivo* tumorigenicity with subsequent apparition of lung metastases when subcutaneously injected into RAG-1 immunodeficient mice. Using human Ki-67 protein as an indicator of metastasis (30), we indeed observed that MT4-MMP over-expression was associated with an increase of both the number and severity of lung metastases. MT1-MMP (39) and pro-MMP-2 (40) over-expressed in cancer cells were already reported to increase experimental lung metastases by intra-venous and intra-cardiac injections, respectively. Here, we demonstrate that MT4-MMP over-expressed in breast cancer cells can lead directly or indirectly to *in vivo* lung metastases after subcutaneous injection. In addition to establishing a new association between MT-MMPs and cancer, our MT4-MMP transfected cells provide a relevant model of lung metastases from primary tumor and involving all steps

implicated in metastatic dissemination such as intravastion, extravasation, and migration (41). Further studies are required to determine which steps of cancer progression are affected by MT4-MMP.

The molecular mechanisms of MT4-MMP action in tumor progression are unknown. Its localization at the cell surface raised the possibility that it controls pericellular proteolysis and participates directly or indirectly to intracellular signaling events. Alternatively, MT4-MMP could be involved in tissue remodeling associated to tumor growth and metastatic spread of cancer cells. In this context, it is worth noting that a role for MT4-MMP in cartilage aggrecanolysis through ADAMTS-4 activation has been described (22). In addition, interleukine-1 (IL-1) has been shown to induce MT4-MMP with subsequent processing of ADAMTS-4 in IL-1-mediated aggrecanolysis of bovine cartilage (23). As assessed by qRT-PCR, no ADAMTS-4 mRNAs were detected in our cultured transfectants or their corresponding *in vivo* xenografts (data not shown). Nevertheless, the lack of ADAMTS-4 detection in established primary tumors does not negate the possibility that an ADAMTS-4/MT4-MMP pathway contributes to earlier steps of cancer development. In addition, we can not exclude a possible implication of this pathway in host-tumor interface in tumor and metastases microenvironments.

Shedding of MT4-MMP offers an alternative way to contribute to biological processes at a distance from the producing cells. Indeed, in accordance with the data of Itoh *et al.* (38), we detected large amounts of MT4-MMP protein shed in the supernatant of cells expressing MT4-MMP (data not shown). In contrast to our and other data previously reported for MT1-MMP (10, 25), the tumor promoting effect of MT4-MMP could not be associated to higher *in vitro* invasive capacities, as assessed in Boyden chamber assays using matrigel and collagen matrices. In addition, consistent with the previous report of English *et al.* (16), MT4-MMP production does not affect the *in vitro* capacity to activate exogenous pro-MMP-2, known to

participate in cell invasion. These observations suggest that MT4-MMP does not contribute to cell invasion through direct extracellular matrix degradation or that it could degrade some substrates via other molecules that are absent *in vitro*. Alternatively, *in vivo* MT4-MMP activities could require other factors, such as for instances, inflammatory mediators or growth factors (16, 19). Our original findings of MT4-MMP protein over-production by epithelial cancerous cells of breast adenocarcinomas and metastastic lymph nodes, in addition to its detection in inflammatory cells [the present study and (16, 19, 42)] extend the putative functions of MT4-MMP and suggest a dual role in both inflammatory responses and cancer processes for MT4-MMP.

The higher *in vivo* tumor growth induced by MT4-MMP expression could not be explained by a direct angiogenic effect as described for MT1-MMP (13, 25). We previously reported that MT1-MMP tumor promoting effect could be linked, at least in part, to an up-regulation of VEGF at a transcriptional levels (12). However, in contrast to MT1-MMP, MT4-MMP over-expressed in breast cancer cells fails to increase *in vitro* VEGF expression. In addition, medium conditioned by transfected cells is not able to enhance *in vitro* angiogenesis in the aortic ring assay. Nevertheless, MT4-MMP production modulates vasculature architecture. In vivo, MT4-MMP induces enlargement of intratumoral blood vessels which were covered by pericytes reflecting their maturity (43). Altogether, our findings suggest that MT4-MMP contribution to cancer progression involves other pathways that those activated by MT1-MMP.

In conclusion, our data clearly demonstrate a pivotal role of MT4-MMP in human breast cancer growth ending up to metastatic dissemination. Both MT1- and MT4-MMPs contribute to cancer progression, but their mechanisms of action are divergent. These findings have direct implication for development of new anti-cancer strategies by highlighting the importance to target different MT-MMPs.

ACKNOWLEGEMENTS

We acknowledge F. Olivier, N. Lefin, M-L Alvarez, G. Roland, I. Dasoul, P. Gavitelli and E. Feyereisen for their technical help. This work was supported by grants from the “Communauté française de Belgique” (Actions de Recherches Concertées), the Commission of European Communities (FP5 and FP6), the “Fonds de la Recherche Scientifique Médicale”, the “Fonds National de la Recherche Scientifique” (F.N.R.S., Belgium), the “Fédération Belge Contre le Cancer”, the “Fonds spéciaux de la Recherche” (University of Liège), the “Centre Anticancéreux près l'Université de Liège”, the “Fortis Banque Assurances”, the “Fondation Léon Fredericq” (University of Liège), the D.G.T.R.E. from the “Région Wallonne”, the “Fonds d’Investissements de la Recherche Scientifique” (F.I.R.S., CHU, Liège, Belgium), the Interuniversity Attraction Poles Programme - Belgian Science Policy (Brussels, Belgium). V.C. is a recipient of a grant from FNRS-Télévie; E.M., C.G. and C.M. are Research Associates and F.v.d.B. is Senior Research Associate, all from FNRS (Belgium). W.R.E. is an Intermediate Fellow of the British Heart Foundation and GM is supported by Cancer Research-UK and the Medical Research Council, UK.

REFERENCES

1. Egeblad M, Werb Z. New functions for the matrix metalloproteinases in cancer progression. Nat Rev Cancer 2002;2:161-74.

2. Overall CM, Lopez-Otin C. Strategies for MMP inhibition in cancer: innovations for the post-trial era. Nat Rev Cancer 2002;2:657-72.

3. Noel A, Maillard C, Rocks N et al. Membrane associated proteases and their inhibitors in tumour angiogenesis. J Clin Pathol 2004;57:577-84.

4. Folgueras AR, Pendas AM, Sanchez LM, Lopez-Otin C. Matrix metalloproteinases in cancer: from new functions to improved inhibition strategies. Int J Dev Biol 2004;48:411-24.

5. Zucker S, Pei D, Cao J, Lopez-Otin C. Membrane type-matrix metalloproteinases (MT-MMP). Curr Top Dev Biol 2003;54:1-74.

6. Sato H, Takino T, Okada Y et al. A matrix metalloproteinase expressed on the surface of invasive tumour cells. Nature 1994;370:61-5.

7. Sabeh F, Ota I, Holmbeck K et al. Tumor cell traffic through the extracellular matrix is controlled by the membrane-anchored collagenase MT1-MMP. J Cell Biol 2004;167:769-81.

8. Sounni NE, Noel A. Membrane type-matrix metalloproteinases and tumor progression. Biochimie 2005;87:329-42.

9. Handsley MM, Edwards DR. Metalloproteinases and their inhibitors in tumor angiogenesis. Int J Cancer 2005;115:849-60.

10. Hotary KB, Allen ED, Brooks PC, Datta NS, Long MW, Weiss SJ. Membrane type I matrix metalloproteinase usurps tumor growth control imposed by the three-dimensional extracellular matrix. Cell 2003;114:33-45.

11. Seiki M, Koshikawa N, Yana I. Role of pericellular proteolysis by membrane-type 1 matrix metalloproteinase in cancer invasion and angiogenesis. Cancer Metastasis Rev 2003;22:129-43.

12. Sounni NE, Roghi C, Chabottaux V et al. Up-regulation of VEGF-A by active MT1-MMP through activation of Src-tyrosine kinases. J Biol Chem 2004;279:13564-74.

13. Deryugina EI, Soroceanu L, Strongin AY. Up-regulation of vascular endothelial growth factor by membrane-type 1 matrix metalloproteinase stimulates human glioma xenograft growth and angiogenesis. Cancer Res 2002;62:580-8.

14. Strongin AY, Collier I, Bannikov G, Marmer BL, Grant GA, Goldberg GI. Mechanism of cell surface activation of 72-kDa type IV collagenase. Isolation of the activated form of the membrane metalloprotease. J Biol Chem 1995;270:5331-8.

15. Morrison CJ, Butler GS, Bigg HF, Roberts CR, Soloway PD, Overall CM. Cellular activation of MMP-2 (gelatinase A) by MT2-MMP occurs via a TIMP-2-independent pathway. J Biol Chem 2001;276:47402-10.

16. English WR, Puente XS, Freije JM et al. Membrane type 4 matrix metalloproteinase (MMP17) has tumor necrosis factor-alpha convertase activity but does not activate pro-MMP2. J Biol Chem 2000;275:14046-55.

17. English WR, Velasco G, Stracke JO, Knauper V, Murphy G. Catalytic activities of membrane-type 6 matrix metalloproteinase (MMP25). FEBS Lett 2001;491:137-42.

18. Velasco G, Cal S, Merlos-Suarez A et al. Human MT6-matrix metalloproteinase: identification, progelatinase A activation, and expression in brain tumors. Cancer Res 2000;60:877-82.

19. Puente XS, Pendas AM, Llano E, Velasco G, Lopez-Otin C. Molecular cloning of a novel membrane-type matrix metalloproteinase from a human breast carcinoma. Cancer Res 1996;56:944-9.

20. Nuttall RK, Pennington CJ, Taplin J et al. Elevated membrane-type matrix metalloproteinases in gliomas revealed by profiling proteases and inhibitors in human cancer cells. Mol Cancer Res 2003;1:333-45.

21. Riddick AC, Shukla CJ, Pennington CJ et al. Identification of degradome components associated with prostate cancer progression by expression analysis of human prostatic tissues. Br J Cancer 2005;92:2171-80.

22. Gao G, Plaas A, Thompson VP, Jin S, Zuo F, Sandy JD. ADAMTS4 (aggrecanase-1) activation on the cell surface involves C-terminal cleavage by glycosylphosphatidyl inositol-anchored membrane type 4-matrix metalloproteinase and binding of the activated proteinase to chondroitin sulfate and heparan sulfate on syndecan-1. J Biol Chem 2004;279:10042-51.

23. Patwari P, Gao G, Lee JH, Grodzinsky AJ, Sandy JD. Analysis of ADAMTS4 and MT4-MMP indicates that both are involved in aggrecanolysis in interleukin-1-treated bovine cartilage. Osteoarthritis Cartilage 2005;13:269-77.

24. Kajita M, Kinoh H, Ito N et al. Human membrane type-4 matrix metalloproteinase (MT4-MMP) is encoded by a novel major transcript: isolation of complementary DNA clones for human and mouse mt4-mmp transcripts. FEBS Lett 1999;457:353-6.

25. Sounni NE, Devy L, Hajitou A et al. MT1-MMP expression promotes tumor growth and angiogenesis through an up- regulation of vascular endothelial growth factor expression. FASEB J 2002;16:555-64.

26. Labarca C, Paigen K. A simple, rapid, and sensitive DNA assay procedure. Anal Biochem 1980;102:344-52.

27. Blacher S, Devy L, Burbridge MF et al. Improved quantification of angiogenesis in the rat aortic ring assay. Angiogenesis 2001;4:133-42.

28. Noel A, Pauw-Gillet MC, Purnell G, Nusgens B, Lapiere CM, Foidart JM. Enhancement of tumorigenicity of human breast adenocarcinoma cells in nude mice by matrigel and fibroblasts. Br J Cancer 1993;68:909-15.

29. Maillard C, Jost M, Romer MU et al. Host plasminogen activator inhibitor-1 promotes human skin carcinoma progression in a stage-dependent manner. Neoplasia 2005;7:57-66.

30. Scholzen T, Gerdes J. The Ki-67 protein: from the known and the unknown. J Cell Physiol 2000;182:311-22.

31. Grant GM, Giambernardi TA, Grant AM, Klebe RJ. Overview of expression of matrix metalloproteinases (MMP-17, MMP-18, and MMP-20) in cultured human cells. Matrix Biol 1999;18:145-8.

32. Pedersen TX, Pennington CJ, Almholt K et al. Extracellular protease mRNAs are predominantly expressed in the stromal areas of microdissected mouse breast carcinomas. Carcinogenesis 2005;26:1233-40.

33. Bisson C, Blacher S, Polette M et al. Restricted expression of membrane type 1-matrix metalloproteinase by myofibroblasts adjacent to human breast cancer cells. Int J Cancer 2003;105:7-13.

34. Gilles C, Polette M, Seiki M, Birembaut P, Thompson EW. Implication of collagen type I-induced membrane-type 1-matrix metalloproteinase expression and matrix metalloproteinase-2 activation in the metastatic progression of breast carcinoma. Lab Invest 1997;76:651-60.

35. Szabova L, Yamada SS, Birkedal-Hansen H, Holmbeck K. Expression pattern of four membrane-type matrix metalloproteinases in the normal and diseased mouse mammary gland. J Cell Physiol 2005;205:123-32.

36. Maquoi E, Frankenne F, Baramova E et al. Membrane type 1 matrix metalloproteinase-associated degradation of tissue inhibitor of metalloproteinase 2 in human tumor cell lines. J Biol Chem 2000;275:11368-78.

37. Remacle AG, Rozanov DV, Baciu PC, Chekanov AV, Golubkov VS, Strongin AY. The transmembrane domain is essential for the microtubular trafficking of membrane type-1 matrix metalloproteinase (MT1-MMP). J Cell Sci 2005;118:4975-84.

38. Itoh Y, Kajita M, Kinoh H, Mori H, Okada A, Seiki M. Membrane type 4 matrix metalloproteinase (MT4-MMP, MMP-17) is a glycosylphosphatidylinositol-anchored proteinase. J Biol Chem 1999;274:34260-6.

39. Tsunezuka Y, Kinoh H, Takino T et al. Expression of membrane-type matrix metalloproteinase 1 (MT1-MMP) in tumor cells enhances pulmonary metastasis in an experimental metastasis assay. Cancer Res 1996;56:5678-83.

40. Tester AM, Waltham M, Oh SJ et al. Pro-matrix metalloproteinase-2 transfection increases orthotopic primary growth and experimental metastasis of MDA-MB-231 human breast cancer cells in nude mice. Cancer Res 2004;64:652-8.

41. Kang Y. Functional genomic analysis of cancer metastasis: biologic insights and clinical implications. Expert Rev Mol Diagn 2005;5:385-95.

42. Gauthier MC, Racine C, Ferland C et al. Expression of membrane type-4 matrix metalloproteinase (metalloproteinase-17) by human eosinophils. Int J Biochem Cell Biol 2003;35:1667-73.

43. Jodele S, Chantrain CF, Blavier L et al. The contribution of bone marrow-derived cells to the tumor vasculature in neuroblastoma is matrix metalloproteinase-9 dependent. Cancer Res 2005;65:3200-8.

Clones	A) Incidence of lung metastasis					B) Average number of lung metastatic nodules/section (mean [range])					
			Severity of metastasis			Severity of metastasis					
	Incidence n/n	(%)	1°	2°	3°	1°		2°		3°	
M2	5/5	(100%)	5/5	1/5	0/5	19.4	[7-46]	0.2	[0-1]	0	-
M3	5/5	(100%)	5/5	5/5	3/5	75	[18-169]	86.4	[5-231]	13	[0-43]
M10	5/5	(100%)	5/5	1/5	2/5	93.8	[4-416]	80.2	[0-401]	7	[0-34]
M14	5/5	(100%)	5/5	4/5	2/5	82	[5-309]	41.2	[0-108]	2	[0-8]
C4	0/5	(0%)	0/5	0/5	0/5	0	-	0	-	0	-
C12	2/5	(40%)	2/5	2/5	0/5	14.2	[0-68]	4	[0-19]	0	-
C14	3/5	(60%)	3/5	2/5	0/5	4.2	[0-19]	0.8	[0-3]	0	-
C15	5/5	(100%)	5/5	2/5	0/5	7	[2-15]	0.4	[0-1]	0	-

Table I. Effect of MT4-MMP on incidence and severity of lung metastasis in RAG-1 -/- mice bearing subcutaneous tumors of MDA-MB-231 clones. Four MDA-MB-231 clones transfected with MT4-MMP (clones M) or with vector control (clones C) were subcutaneously injected (1 x 10^6 cells/injection) into RAG-1 -/- mice (5 mice/clone). Mouse lung tissue sections were immuno-stained for human KI-67 protein. Metastatic foci were counted in 65 histological fields (5 mice/clone) at 200-fold magnification. The incidence of metastasis (*A*) is expressed as the percentage of mice with detectable metastatic cells in the lungs. Severity of metastasis was scored as follows: minimal (1° = metastatic nodule involving less than 3 stained cells), medium (2° = metastatic nodule composed of 3 to 20 stained cells), or extensive involvement (3° = metastatic nodule including more than 20 stained cells). Cells expressing MT4-MMP showed a significant increase of metastasis incidence ($P < 0.001$). Number and severity of metastasis is expressed as the mean with the range for each transfectant groups (*B*).

LEGEND TO FIGURES

Figure 1. Expression of MT4-MMP in human breast adenocarcinomas. *A)*, Relative mRNA expression level of MT4-MMP in 63 breast cancer and 21 normal breast samples assessed by qRT-PCR. Results are expressed as ratios of MT4-MMP mRNA to 18S rRNA levels. Bars represent median. *B)*, Immunohistochemical detection of MT4-MMP in human breast adenocarcinoma, normal breast, metastatic and normal lymph nodes. Breast tumor sections ("breast carcinoma") displayed a strong and extensive MT4-MMP production in tumor cells *(t)*, but not in the surrouding stroma *(s).White arrow:* myoepithelial cells; *a:* adipocytes; *s:* stroma; *t:* tumor cells; *l:* lymphocytes; *d:* ducts; *m:* metastatic cells; *ca:* node capsule; *gc:* germinal center; *co:* cortex. Photomicrographs at 400 fold-magnification (scale bar = 50 µm) and 100 fold-magnification (scale bar = 200 µm) for left and right panels, respectively. *C)*, Quantification of MT4-MMP immunostaining. Average staining density (higher panel) and staining intensity (lower panel) were determined on 25 representative sections of each group as described in Material and Methods section. Error bars represent SE (*** $P < 0.001$).

Figure 2. Analysis of MT4-MMP expression in MDA-MB-231 clones stably transfected with MT4-MMP cDNA (M2, M3, M10, M14) or with pcDNA3-*neo* control vector (C4, C12, C14, C15). *A)*, RT-PCR analysis of MT4-MMP mRNA level. Expression of 28S rRNA is shown as loading control. *B)*, Western blot analysis of MT4-MMP protein. Total protein extracts of clones were analyzed using an anti-human MT4-MMP sheep polyclonal antibody raised against MT4-MMP catalytic domain. Actin production level in transfectants is shown as loading control.

Figure 3. Characterization of *in vitro* and *in vivo* properties of four MDA-MB-231 clones stably transfected with MT4-MMP cDNA (black symbols, continued lines, clones M) or with

pcDNA3-*neo* control vector (white symbols, dotted lines, clones C). *A)*, *In vitro* growth curves of transfectants. Clones were seeded in triplicate in 24-well plates and harvested each day for DNA content evaluation. Results, expressed as mean of DNA concentration of triplicates +/- SE, are those of one representative experiment out of 3. *B)* and *C)*, *In vivo* tumor growth curves of the transfectants. Clones were subcutaneously injected into RAG-1 -/- mice in three independent assays and tumor volumes were assessed as described in Material and Methods. Data shown are those of 2 representative independent experiments, in which MT4-MMP clones (M2, M3, M14 in *B*; M2, M3, M10 in *C*) and control clones (C4, C12, C15 in *B*; C4, C14 in *C*) were tested. Results are expressed as mean of tumor volumes for each experimental group +/- SE (*** $P < 0.001$; ** $P < 0.01$; * $P < 0.05$).

Figure 4. Immunohistochemical analysis of primary tumors. Tumors were induced by subcutaneous injection of MT4-MMP transfected MDA-MB-231 clones (MT4 clones, left side) or control clones (CTR clones, right side) into RAG-1 -/- mice. Tumor sections were immunostained by using antibodies raised against: *A)*, MT4-MMP; *B)*, von Willebrand factor (vWF); *C)*, α- smooth muscle actin (SMA). Photomicrographs at 200 fold-magnification (scale bar = 100 µm). *B* and *C* represent serial sections for both experimental groups.

Figure 5. Immunodetection and quantification of lung metastases. MDA-MB-231 clones expressing MT4-MMP (MT4 clones, left side) or not (CTR clones, right side) were subcutaneously injected into RAG-1 -/- mice (5 to 6 mice/clones) in two independent assays. At day 45, lungs were collected, formalin-fixed and parafin-embedded. *A)* and *B)*, Metastatic nodules were immunodetected in lung tissue sections with an antibody raised against human Ki-67 protein and scored 1° *(white arrow)*, 2° *(grey arrow)* or 3° *(black arrow)* as described in Material and Methods. *C)*, Immunostaining analysis confirmed MT4-MMP production in

metastases induced by MT4-MMP transfected cells (left side). Photomicrographs at 100 fold-magnification in *A* (scale bar = 200 µm) or 200-fold magnification in *B* and *C* (scale bar = 100 µm). *B* and *C* represent serial sections for both experimental groups. *bv:* blood vessel. *D)*, For each clone, metastatic foci were counted in 65 histological fields at 200-fold magnification. Severity of metastasis was scored as illustrated in panel *A*. Results are expressed as the average number of metastatic nodules detected per mice for both experimental groups. Error bars represent SE. Cells transfected with MT4-MMP show a significant increase in number and severity of metastasis. Control clones never produced score 3° metastasis (*** $P < 0.001$ and * $P < 0.05$).

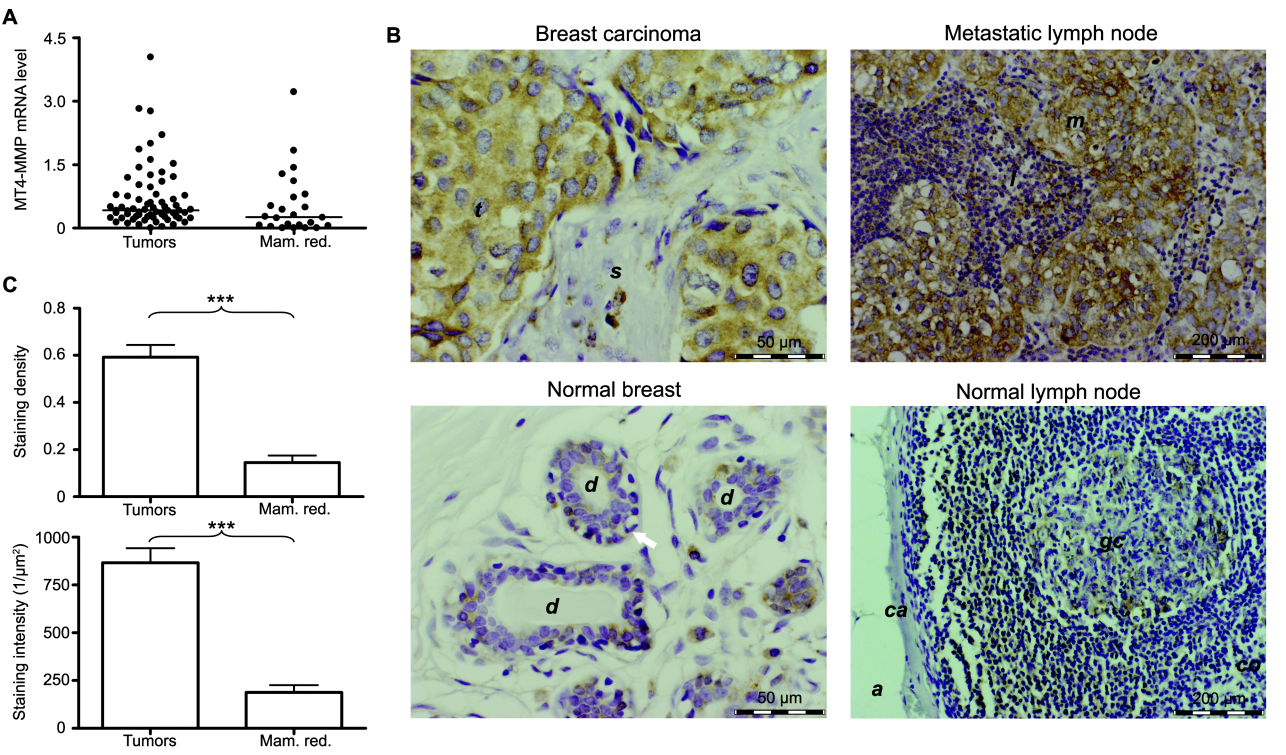
A
MT4-MMP mRNA level
4.5
3.0
1.5
0
Tumors
Mam. red.
B
Breast carcinoma
t
s
50 µm
Metastatic lymph node
m
l
200 µm
Normal breast
d
d
d
50 µm
Normal lymph node
gc
ca
a
cp
200 µm
C
Staining density
0.8
0.6
0.4
0.2
0
***
Tumors
Mam. red.
Staining intensity (1/µm²)
1000
750
500
250
0
***
Tumors
Mam. red.

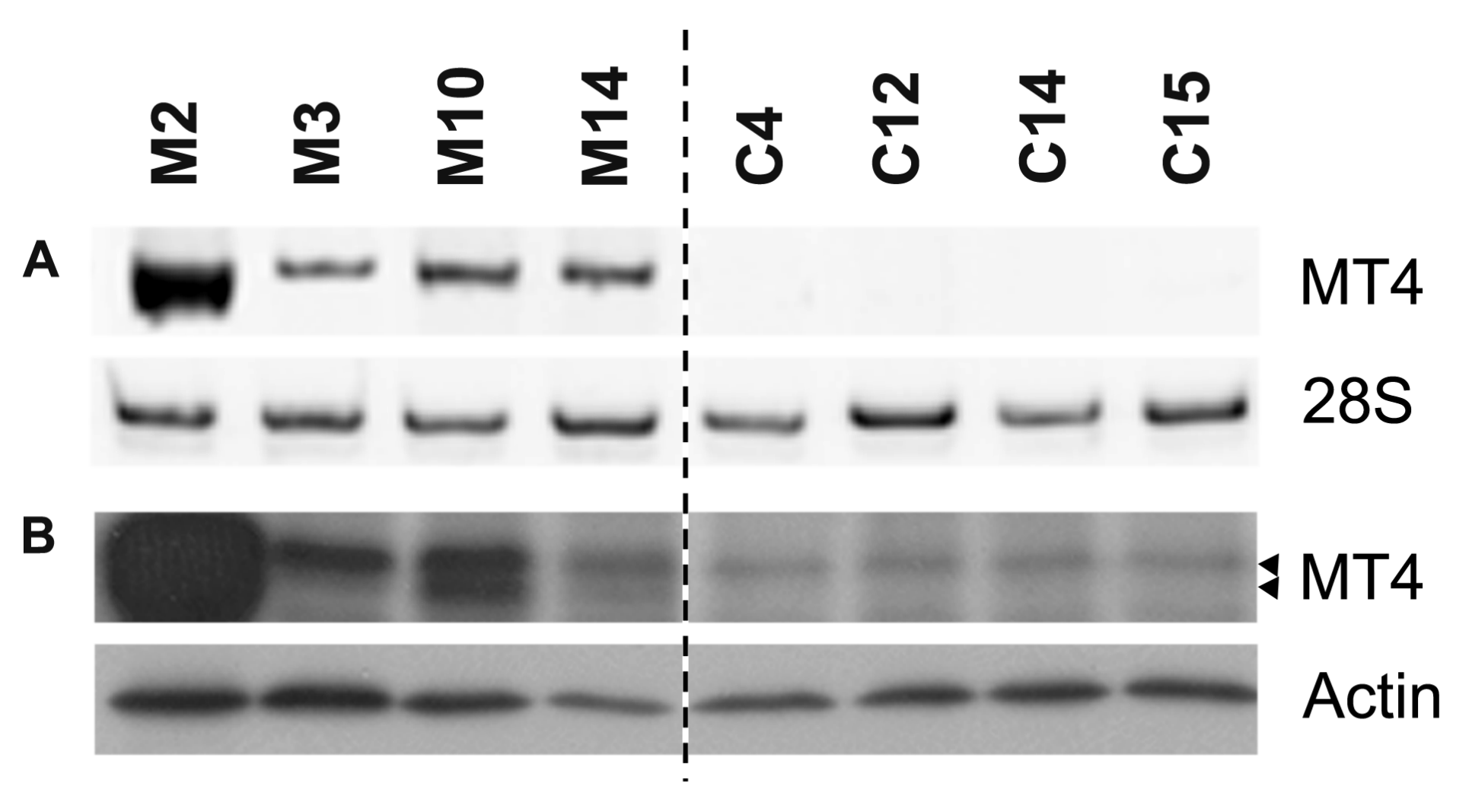
M2
M3
M10
M14
C4
C12
C14
C15
A
MT4
28S
B
MT4
Actin

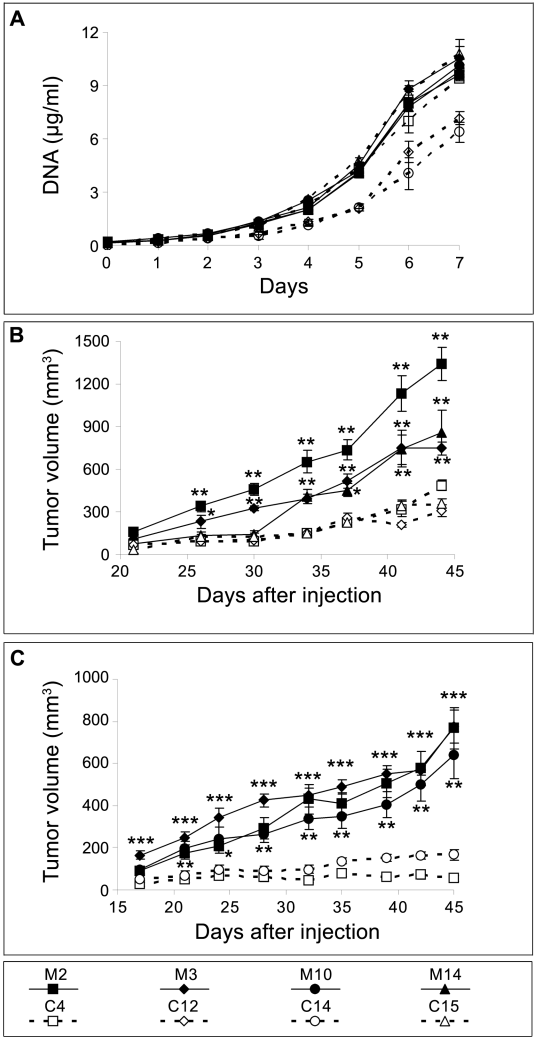
A
DNA (µg/ml)
Days
B
Tumor volume (mm3)
Days after injection
C
Tumor volume (mm3)
Days after injection
M2
M3
M10
M14
C4
C12
C14
C15

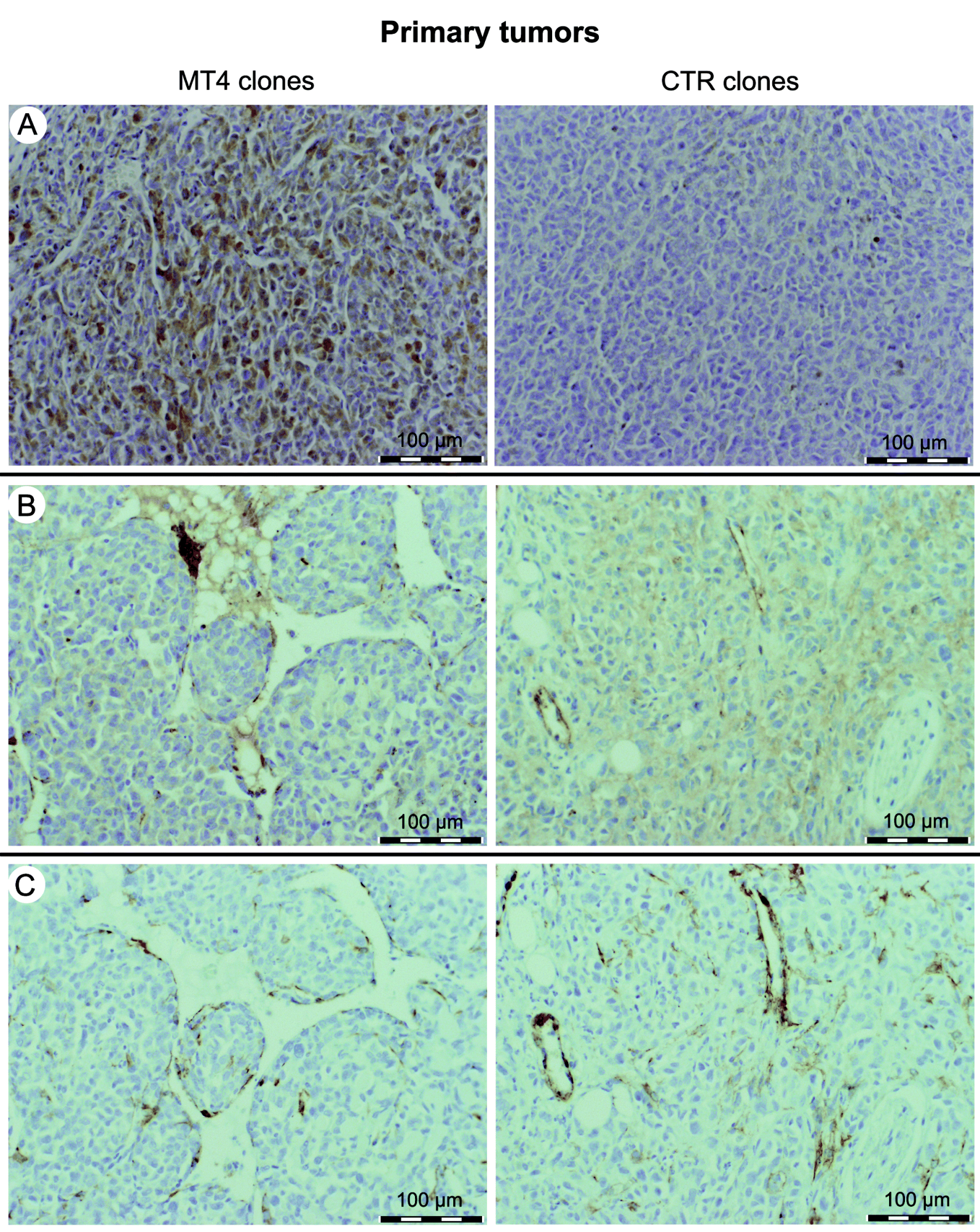
Primary tumors
MT4 clones
CTR clones
A
100 µm
100 µm
B
100 µm
100 µm
C
100 µm
100 µm

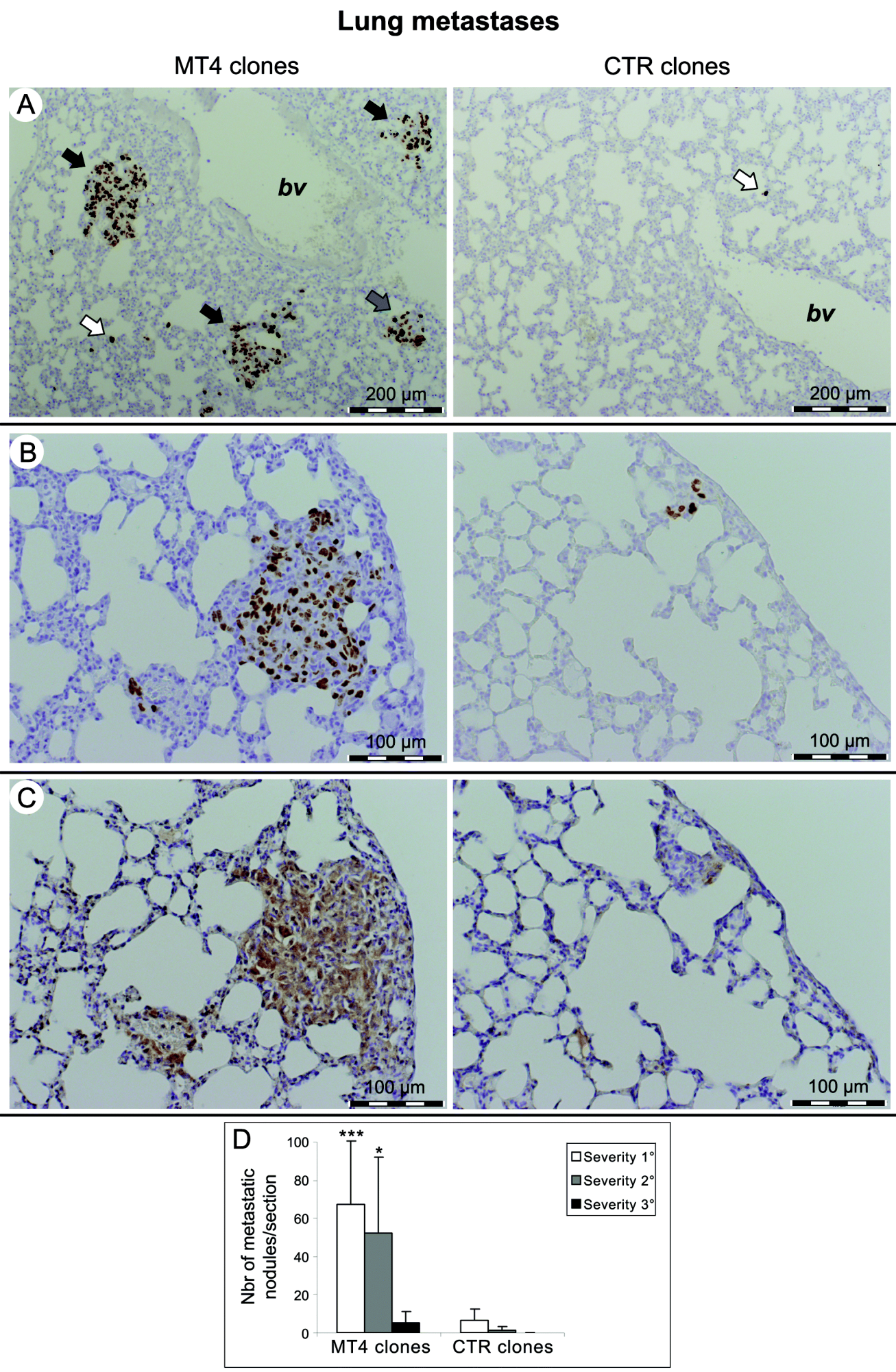
Lung metastases
MT4 clones
CTR clones
A
bv
200 µm
bv
200 µm
B
100 µm
100 µm
C
100 µm
100 µm
D
Nbr of metastatic nodules/section
100
80
60
40
20
0
***
*
MT4 clones
CTR clones
Severity 1°
Severity 2°
Severity 3°